The anisotropy of free path in a vibro-fluidized granular gas*

Yifeng Mei(梅一枫)[1], Yanpei Chen(陈延佩)[1,†], Wei Wang(王维)[1], and Meiying Hou(厚美瑛)[2]

[1] State Key Laboratory of Multiphase Complex Systems, Institute of Process Engineering, Chinese Academy of Sciences, Beijing 100190, China
[2] Key Laboratory of Soft Matter Physics, Beijing National Laboratory for Condense Matter Physics, Institute of Physics, Chinese Academy of Sciences, Beijing 100190, China

(Received 15 March 2016; revised manuscript received 18 April 2016; published online 25 June 2016)

The free path of a vibro-fluidized two-dimensional (2D) inelastic granular gas confined in a rectangular box is investigated by 2D event-driven molecular simulation. By tracking particles in the simulation, we analyze the local free path. The probability distribution of the free path shows a high tail deviating from the exponential prediction. The anisotropy of the free path is found when we separate the free path to x and y components. The probability distribution of y component is exponential, while x component has a high tail. The probability distribution of angle between the relative velocity and the unit vector joined two particle centers deviates from the distribution of two random vectors, indicating the existence of the dynamic heterogeneities in our system. We explain these results by resorting to the kinetic theory with two-peak velocity distribution. The kinetic theory agrees well with the simulation result.

Keywords: free path, granular gases, two-peak velocity distribution

PACS: 45.70.–n, 51.10.+y, 45.70.Mg **DOI:** 10.1088/1674-1056/25/8/084501

1. Introduction

Granular gases,[1,2] known as rapid granular flows, refer to the fact that macroscopic grains interact via instantaneous inelastic collisions. The granular gas is widespread not only in nature, such as interstellar dust, planetary rings, and avalanches, but also in the industry where the granular media are fluidized by shear, vibration or gravity. Given the presence of inelastic collision, it is different from the molecular gas by nature, featuring non-Maxwell velocity distribution, inhomogeneous density distribution (clustering and patterns), and lack of energy equipartition.[3,4] In particular, the velocity distribution of granular gases shows exponential distribution as confirmed in experiments[5–7] and simulations.[8] Two peaks of local velocity distribution were further found in simulation[8–10] and also in micro-gravity experiments.[11,12] In greater detail, the local velocity distributions of the vibration direction show two peaks in the marginal layer, melting into one peak in the box center, as demonstrated by the relevant skewness. All these suggest a granular gas may not reach fast local equilibrium. In order to study such non-equilibrium systems, we need to start from certain basic issues. The collision statistics, especially free path length or free flight time, which is useful in estimation of transport coefficient and the energy loss for granular gases, is supposed to be one of them.

The mean free path[13,14] is normally applied to characterize free path lengths. It is defined as the average distance that a molecule travels between successive collisions. It is a critical criterion that determines whether the granular dynamics can be described by the hydrodynamics or not[13,15] for granular gases. Besides, it can be used to calculate the transport property for granular media, such as viscosity.[8,14] The classical mean free path of molecular gases could be derived strictly from the Maxwell velocity distribution. Grossman *et al.*[16] gave mean free path expressions for granular gases in the low and high density limits in nearly elastic conditions. The low density expression is the same as the mean free path of molecular gases, while the high density one is deduced based on the close-packing density. In the above derivation, an important assumption is the molecular chaos (Stosszahlansatz), which supposes the velocity between two colliding particles is uncorrelated. Further, Brey *et al.*[8] used the local mean free path replacing the coordinate to obtain the spatial profiles of temperature for a granular gas fluidized by a vibrating wall and a reflecting one, then built a relationship between the velocity of the wall and the hydrodynamic profiles.

However, the free path in dissipated granular gases is different from that in elastic gases,[17–19] since the assumption of molecular chaos is based on the local equilibrium. For example, Blair and Kudrolli[17] reported an experiment of collision statistics of vibro-fluidized granular particles on an inclined plane. The distribution of the free path lengths does not follow a simple exponential form on density which is derived by the basic kinetic theory. Visco *et al.*[18] studied the probability distribution of the free flight time and the number of collisions in a hard sphere gas at equilibrium with three simulation methods, the Molecular Dynamics, Direct Simulation

*Project supported by the National Basic Research Program of China (Grant No. 2012CB215003), the National Natural Science Foundation of China (Grant No. 91334204), the Fund from the Chinese Academy of Sciences (Grant No. XDA07080100), and China Postdoctoral Science Foundation (Grant No. 2014M561071).

†Corresponding author. E-mail: ypchen@ipe.ac.cn

Monto Carlo, and Monte Carlo family. The results showed that the number of collision deviates from Poissonian statistics, whereas the probabilistic ballistic annihilation model[19] was found to be able to well explain the simulation results. Tan and Goldhirsch[20–23] studied the mean free path in a uniform shear flow, elucidating that the dimensional shear rate is not small even for strong dissipation and the 'true' mean free path is larger than that in equilibrium state. It is worth noting that the non-equilibrium features of dissipative granular gases are not fully considered in these works. For example, the two-peak local velocity distribution, as discussed above, has not been taken into account in their analysis.

To introduce the non-equilibrium feature into the analysis of the mean free path, in this work, we first present the event-driven molecular simulation method, in which the two-peak local velocity distributions are emphasized. Then the spacial profiles and the probability distribution of free path lengths, the probability of collision angles and the probability distribution of the components of free path lengths are presented. Based on two-peak velocity distribution model, the kinetic expression of the local free path is finally given. Comparison between our theory and simulation results are also discussed.

2. Model and simulation analysis

Granular gases consisting of N inelastic 2D particles (disks) with monodisperse diameter $d = 1$ and mass $m = 1$ are studied in a rectangular box. Figure 1 presents the schematic illustration of our simulation. The idealized sawtooth manners presented in Ref. [9] are adopted for initial distribution of disks in y direction. If the velocities of the disks before collision are $\boldsymbol{v}_1$ and $\boldsymbol{v}_2$ and after collision $\boldsymbol{v}_1'$ and $\boldsymbol{v}_2'$, let $\boldsymbol{v}_{12}$ and $\boldsymbol{v}_{12}'$ be the relative velocities of the disks before and after collision, then an inelastic collision satisfies that

$$\boldsymbol{k}\cdot\boldsymbol{v}_{12}' = -e(\boldsymbol{k}\cdot\boldsymbol{v}_{12}), \tag{1}$$

where $\boldsymbol{k}$ denotes the unit vector directed from the center of the second disk to that of the first one, e is the restitution coefficient with the range [0, 1].

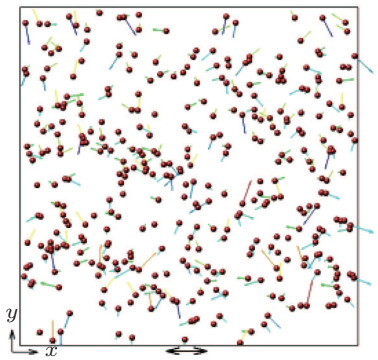

Fig. 1. (color online) The schematic illustration of our simulations.[10]

To drive the disks, we adopt the method used in Ref. [9], a sawtooth driving wall with vanishing amplitude A and diverging frequency ν in x direction. So each disk colliding with the wall has the post-collision velocity:

$$\boldsymbol{v}' = \boldsymbol{v} + \Delta\boldsymbol{v}_{pw}, \tag{2}$$

where

$$\Delta\boldsymbol{v}_{pw} = (-2v_x \pm v_{\text{drive}})\boldsymbol{k}_x, \tag{3}$$

and $\boldsymbol{k}_x$ is the x component of $\boldsymbol{k}$. To obtain the asymptotic dynamics of these fitting parameters, we use a coarse graining method.[23] The coarse graining function, $\Phi(\boldsymbol{R})$, defines spatial "windows" with width $\delta x = L_x/270$ (270 strips are fixed in all simulations, so δx are changed according to L_x) along x direction and length $\delta y = L_y$ along y direction. The "window" moves step-by-step along y direction (here, the step size is 1), which means "windows" overlapping one with another. All the particles appearing in one "window " count towards the total amount. In our case, there are 270 windows in x axis. For instance, when $L_x = 300$, $\Phi(\boldsymbol{R})$ begins from $x \subseteq [0\ 30]$, then [1 31], ..., until [270 300]. It needs to be emphasized that our results are obtained from the simulation. When one disk collides with another, its positions are stored. Once the next collision happens, the free path can be calculated directly from the last collision position.

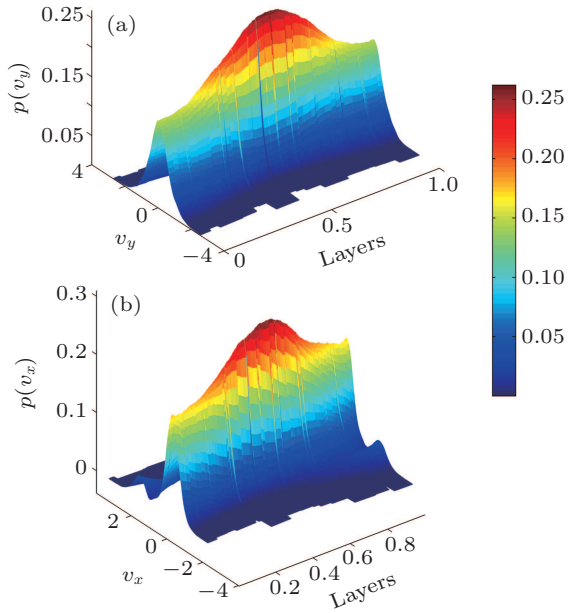

Fig. 2. (color online) Three-dimensional (3D) probability distribution of the velocity. $L_x = L_y = 300$, $e = 0.9$, $N = 1000$, $V_{\text{driven}} = 10$.

As in Ref. [11], we measure the local velocity distribution in each window which moves from the left side to the right side of the box. The three-dimensional plot of the local velocity distributions $p(v_x)$ and $p(v_y)$ are illustrated for an inelastic case with $N = 1000$, $e = 0.9$ in Fig. 2. Our simulation results are consistent with the experimental[11] and previous

simulation results.[8–10] Anisotropy refers to the property of the directional dependence, which could be clearly observed in Fig. 2. $p(v_y)$ in all the layers show symmetry, while two peaks appear in the boundary layer for $p(v_x)$, one corresponding to positive velocity and the other negative, then melt to one peak when the location moves to the box center. The superposition of two Maxwellian distributions can be supposed to describe this local velocity distribution in such system as in our previous work.[12]

3. The distribution of free path lengths

For a molecule moving in an irregular, zigzag path, the mean free path, λ, is expressed in terms of the number density and diameter. For granular gases, two situations[16] are usually included for two-dimensional nearly elastic hard disk gases: in the low density limit, λ is given by

$$\lambda_{\rm l} = \frac{1}{\sqrt{8}\rho d} \tag{4}$$

and in the high density limit, it has

$$\lambda_{\rm h} = \frac{\rho_{\rm c} - \rho}{2\rho_{\rm c}} d, \tag{5}$$

where $\rho_{\rm c}$ is the close packing density given by $\rho_{\rm c} = 2/(\sqrt{3}d^2)$, ρ is the local number density and d is the diameter of the disk. Equation (4) is the same as the molecular dynamic theory.

Both equations (4) and (5) are related to the density, so we firstly show the spacial profiles of the local density in Fig. 3. We could find the local dependence of density on the restitution coefficient. Figure 4 illustrates the spatial profiles of the local free path in our simulation using the coarse graining method for two cases, one is nearly elastic ($e = 0.99$), the other is inelastic ($e = 0.9$). The results from Eq. (4) are also given for comparison. The area fraction is $\phi = \pi d^2 N/4L_xL_y = 0.034$, and the global mean free path calculated from Eq. (4) or the molecular gases is $\lambda_{\rm l} = 1/\sqrt{8}\rho d = 31.8$. It is pretty clear that the local free path deviates from the mean one, especially for the inelastic case. In general, the coarse graining simulation results are closer to the prediction of Eq. (4), but difference still exists especially in the boundary layer. Dissipative collisions cause inhomogeneous distinction of particles and dense accumulation in the central area. Thus λ drops when leaving the boundary. This trend is more significant for the inelastic case of $e = 0.9$.

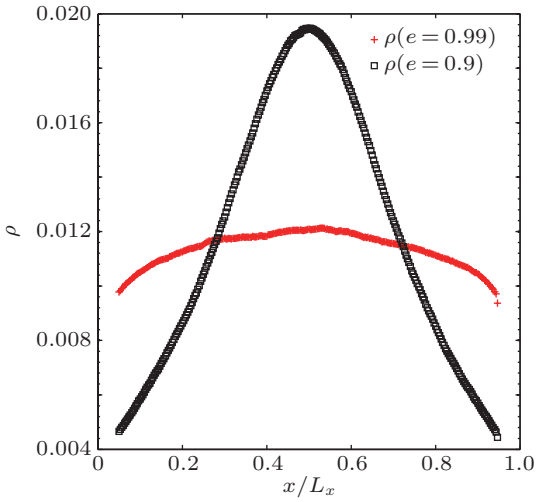

Fig. 3. (color online) The spatial profiles of number density ρ with different restitution coefficient ($e = 0.99$ and $e = 0.9$), $L_x = L_y = 300$, $N = 1000$, $V_{\rm driven} = 5$.

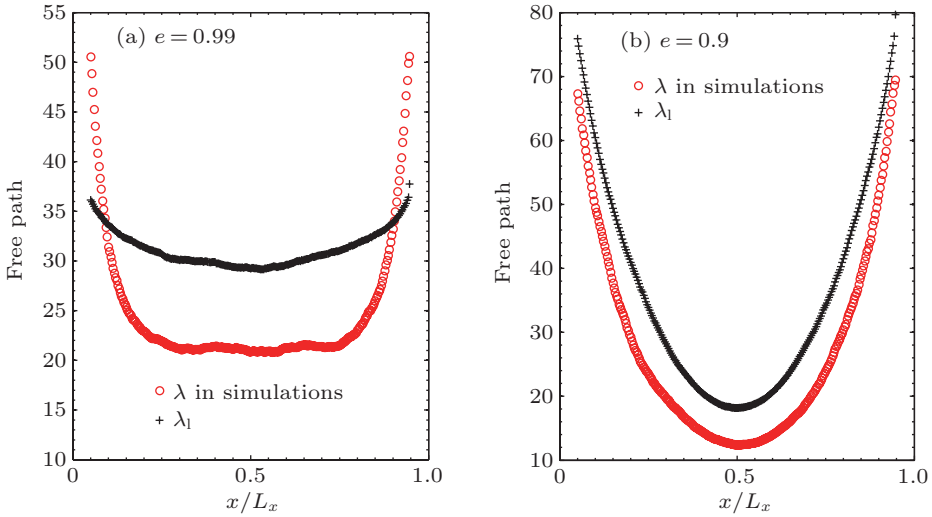

Fig. 4. (color online) The spatial profiles of local free path λ, for (a) $e = 0.99$ and (b) $e = 0.9$. Other parameters are $L_x = L_y = 300$, $N = 1000$, $V_{\rm driven} = 5$.

According to the kinetic theory, the distribution of free paths for nearly elastic particle is given by

$$P(\lambda) = (2\sqrt{2}\phi)\,{\rm e}^{-2\sqrt{2}\phi\lambda}. \tag{6}$$

It indicates that $P(\lambda)$ follows an exponential distribution related to the area fraction. The previous results[17] of inclined plane experiment show $P(\lambda)$ is inconsistent with Eq. (6)

largely. For our case, $P(\lambda)$ decreases with the free path length on semi-log coordinate as presented in Fig. 5. It is pretty clear that our results cannot be described by Eq. (6) either. The inset with double logarithmic coordinates shows this curve and a solid line of exponential fitting. We could find the short path length still follows an exponential distribution, while the longer path length diverges greatly. This is expected because the larger free path involves boundary heating that brings deviation. In Ref. [17], only the central area of the vibrated cell are analyzed, so its boundary effect is omitted. That is why their results could still be fitted with an exponential function.

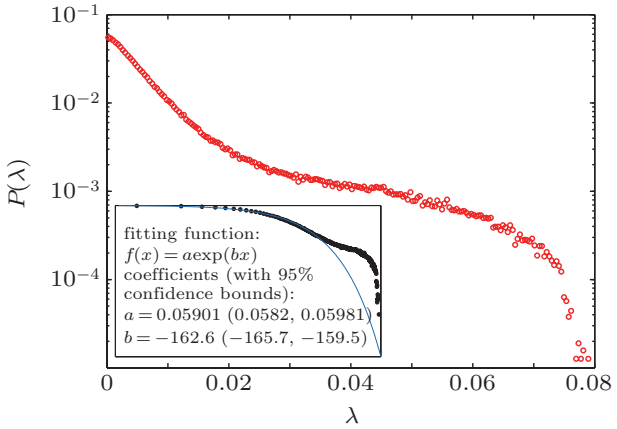

Fig. 5. (color online) The probability distribution of free path lengths $P(\lambda)$, where $e = 0.9$, $L_x = 600$, $L_y = 300$, $N = 1000$, $V_{\text{driven}} = 5$.

Further, we analyze the probability distribution of the angle between the relative velocity, $\boldsymbol{c}_{12}$, and the unit vector joining the centers of two particles, $\boldsymbol{k}$, in Fig. 6. The distribution of angles for two random vectors in α dimensional space[24] is given by

$$P(\theta) = \frac{1}{\sqrt{\pi}} \frac{\Gamma\left(\frac{\alpha}{2}\right)}{\Gamma\left(\frac{\alpha-1}{2}\right)} (\sin(\theta))^{\alpha-2}, \quad \theta \in [0, \pi]. \tag{7}$$

For two-dimensional cases, $P(\theta)$ is constant over $[0, \pi]$, indicating that $P(\theta) = 1/180^\circ = 0.0055$ in angle coordinate. For our case, $P(\theta) = 1/90^\circ = 0.011$ according to Eq. (7). However, our results clearly show angle distribution is not uniform in various restitution coefficients, as shown in Fig. 6. The probability decreases with the collision angle, which means more collisions happen when θ is smaller. If we assume the direction of $\boldsymbol{k}$ is random, then figure 6 implies the relative velocity $\boldsymbol{c}_{12}$ is not isotropic. The probability of direct impact is higher than the oblique impact, implying the existence of the dynamic heterogeneities in our system. In fact, this has already been confirmed in Ref. [10].

Considering the anisotropy due to boundary heating, we further investigate the anisotropic distribution of free path lengths and compare the x and y components of free path as shown in Fig. 7. Here, we have $\lambda = \sqrt{\lambda_x^2 + \lambda_y^2}$. $P(\lambda_y)$ follows the exponential distribution as shown linear in the semi-log coordinate, which is consistent with the kinetic theory argument. However, $P(\lambda_x)$ deviates greatly from the expected. So the distribution of the total free path lengths $P(\lambda)$ is no longer exponential. This clearly results from the boundary effect in x axis. As shown in our previous work,[12] boundary effect leads to two-peak local velocity distribution, and of course leads to anisotropy of the free path lengths.

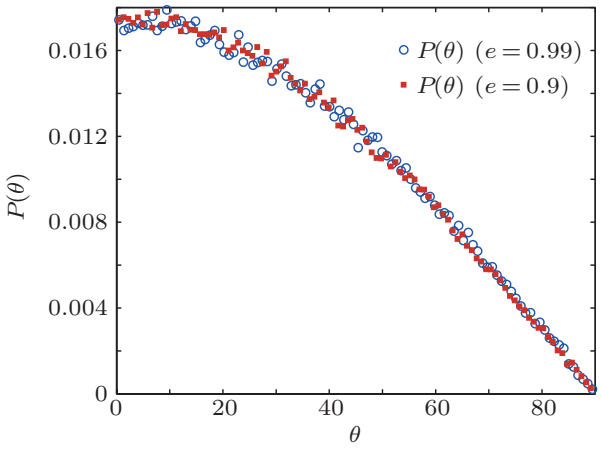

Fig. 6. (color online) The probability of collision angle $P(\theta)$, where θ is the angle between the relative velocity and line of centers of a couple of particles upon collision, and $e = 0.99, 0.9$, $L_x = L_y = 300$, $N = 1000$, $V_{\text{driven}} = 5$.

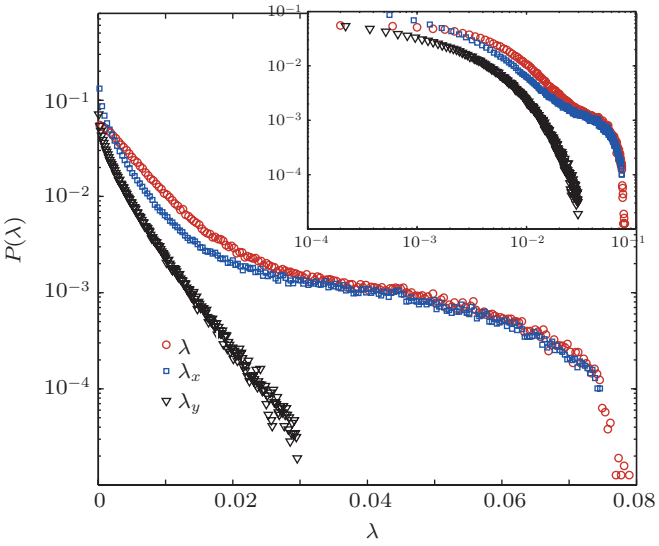

Fig. 7. (color online) The probability distribution of free path lengths $P(\lambda)$ and its x and y components, $P(\lambda_x)$ and $P(\lambda_y)$, where $e = 0.9$, $L_x = 600$, $L_y = 300$, $N = 1000$, $V_{\text{driven}} = 5$ on semi-log coordinate and inset: log–log scale.

4. The kinetic theory description

As presented in Section 2, the non-Maxwellian distribution can be described with a two-peak velocity distribution as shown in Fig. 2, then it is convenient to calculate the local free path according to the kinetic theory and give an explanation[25] based on the two-peak velocity distribution for the longer free path.

We suppose the velocity distribution function is bimodal, which can be written as:

$$f_x(\boldsymbol{c},\boldsymbol{r}) = \frac{n_p m_p}{2\pi T_p}\exp\left[-\frac{m_p(\boldsymbol{c}_p-\boldsymbol{u}_p)^2}{2T_p}\right] + \frac{n_n m_n}{2\pi T_n}\exp\left[-\frac{m_n(\boldsymbol{c}_n-\boldsymbol{u}_n)^2}{2T_n}\right], \quad (8)$$

where subscript p denotes the positive component, while n represents the negative one. T_p and T_n are the granular temperatures defined as $T_p = \langle\sum(v_x^+)^2\rangle$ and $T_n = \langle\sum(v_x^-)^2\rangle$, $\boldsymbol{u}_p$ and $\boldsymbol{u}_n$ are the mean velocities defined as $\boldsymbol{u}_p = \langle v_x^+\rangle$ and $\boldsymbol{u}_n = \langle v_x^-\rangle$. Then, the collision frequency between any of two particles 1 and 2 is

$$N_{ij} = \iint f_{ij}^2(\boldsymbol{c}_{1i},\boldsymbol{r}_i,\boldsymbol{c}_{2j},\boldsymbol{r}_j)(\boldsymbol{c}_{21,ji}\cdot\boldsymbol{k})d_{ij}\mathrm{d}\boldsymbol{k}\mathrm{d}\boldsymbol{c}_{1i}\mathrm{d}\boldsymbol{c}_{2j}, \quad (9)$$

where i and j could be positive or negative components. Let the relative velocity of the particles be

$$\boldsymbol{c}_{ji} = \boldsymbol{c}_j - \boldsymbol{c}_i \quad (10)$$

and the mass center velocity be

$$\boldsymbol{G} = \frac{1}{m_0}(m_j\boldsymbol{c}_j + m_i\boldsymbol{c}_i), \quad (11)$$

where $m_0 = m_i + m_j$, $d_{ij} = (d_i + d_j)/2$. Considering the particle motion is two-dimensional, so

$$\int_{\boldsymbol{c}_{ji}\cdot\boldsymbol{k}>0} \boldsymbol{c}_{ji}\cdot\boldsymbol{k}\mathrm{d}\boldsymbol{k} = 2c_{ji}, \quad (12)$$

where $\boldsymbol{c}_{ji}\cdot\boldsymbol{k} > 0$ is to make sure a collision will happen.

When $\boldsymbol{v}_i$ and $\boldsymbol{v}_j$ are substituted by $\boldsymbol{G}$ and $\boldsymbol{c}_{ji}$, the frequency of collision is expressed as

$$N_{ij} = \iint \frac{2n_i n_j m_i m_j d_{ij}}{(2\pi)^2 T_i T_j} \times \exp(-A\boldsymbol{G}^2 - Dc_{ij}^2 - 2B\boldsymbol{G}\cdot\boldsymbol{c}_{ji} - \boldsymbol{E}\cdot\boldsymbol{G} - \boldsymbol{F}\cdot\boldsymbol{c}_{ji} - H) \times c_{ji}\mathrm{d}\boldsymbol{c}_{ji}\mathrm{d}\boldsymbol{G}. \quad (13)$$

Then expanding it by Taylor series and keeping only the linear terms, the solution of Eq. (13) is

$$N_{ij} = \frac{n_i n_j m_i m_j d_{ij}}{T_i T_j}\frac{\sqrt{\pi}}{4AD^{3/2}}\mathrm{e}^{-H}\left[1+\frac{3B^2}{2AD}\right], \quad (14)$$

where

$$A = \frac{m_i T_j + m_j T_i}{2T_i T_j}, \quad B = \frac{m_i m_j (T_i - T_j)}{2m_0 T_i T_j}, \quad (15)$$

$$D = \frac{m_i m_j (m_i T_i + m_j T_j)}{2m_0^2 T_i T_j}, \quad \boldsymbol{E} = \frac{m_i}{T_i}\boldsymbol{u}_i + \frac{m_j}{T_j}\boldsymbol{u}_j, \quad (16)$$

$$\boldsymbol{F} = \frac{m_i m_j}{m_0}\left(\frac{\boldsymbol{u}_i}{T_i} - \frac{\boldsymbol{u}_j}{T_j}\right), \quad H = \frac{m_i}{2T_i}\boldsymbol{u}_i^2 + \frac{m_j}{2T_j}\boldsymbol{u}_j^2. \quad (17)$$

For our monodisperse case, the masses of species 1 and 2 are equal to each other, then the expression of N_{ij} can be reduced to

$$N_{ij} = \frac{8\sqrt{2\pi}d_{ij}n_i n_j (T_i T_j)^{3/2}}{(T_i+T_j)^{5/2}}\exp\left[-\frac{1}{2}\left(\frac{u_i^2}{T_i}+\frac{u_j^2}{T_j}\right)\right] \times\left[1+\frac{3(T_i-T_j)^2}{2(T_i+T_j)^2}\right]. \quad (18)$$

When $T_i = T_j$ and $\boldsymbol{u}_i = \boldsymbol{u}_j = 0$, the expression reduces to that for the molecular gases mixture in Ref. [26] for two dimensional gas.

Then we can calculate the local free path based on Eq. (18). The one for the positive direction is

$$\lambda_p = n_p\overline{u}_p/(N_{pp}+N_{pn}). \quad (19)$$

So the negative mean free path is

$$\lambda_n = n_n\overline{u}_n/(N_{nn}+N_{pn}). \quad (20)$$

According to the coarse-graining simulation results, $\boldsymbol{u}_p$ and $\boldsymbol{u}_n$ are normally small, especially in the box center. For the sake of simplicity, we assume $\boldsymbol{u}_p = \boldsymbol{u}_n = 0$ and do not take into account the high-order expanded terms in Eq. (18).

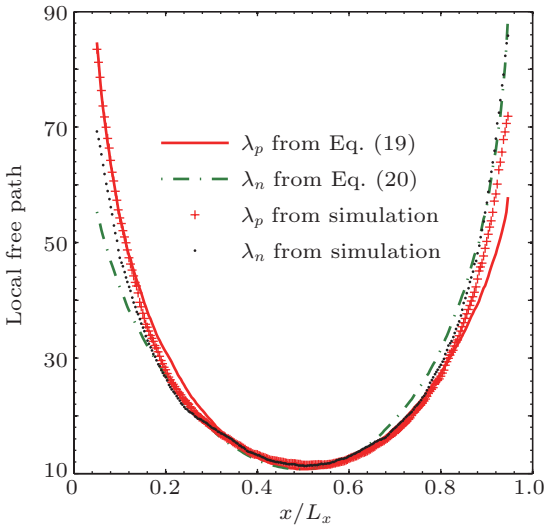

Fig. 8. (color online) Parametric plots of Eq. (19) λ_p and Eq. (20) λ_n, compared with the coarse-graining simulation results with parameters $L_x = L_y = 300$, $e = 0.9$, $N = 1000$, $V_{\text{driven}} = 5$.

Figure 8 compares the local free path from our simulation with that from Eq. (19) and Eq. (20), which shows good agreement. Compared to Fig. 2, the prediction based on the two-peak velocity distribution model is much better than that based on the Maxwellian distribution, showing the effect of the non-equilibrium state in granular gases.

Although equations (19) and (20) better explain the local free path in both positive and negative directions, small deviation still persists in the boundary layer. A possible reason is attributed to inhomogeneous collision angle. From the above deduction, we could find that equation (12) assumes the spatial distribution of all particles are homogeneous, then we

can do spatial integral. However, when one velocity component is greater than the other one, the collision angle becomes smaller. Let us consider an extreme case, when $v_y = 0$, all the particles move in x direction. Then collisions only happen in x direction, the collision angle is zero. In more general cases, $v_y \ll v_x$, then collisional cylindrical volume swept out by the sphere will not be zig–zag but cling to x axis. Equation (12) does not take into account such inhomogeneous collision angle.

In all, our results evidence another mesoscopic nature of the granular gas. As mentioned in the shear granular system,[20] a mesoscopic system is different from the macroscopic one, particularly in average properties, so is the mean free path. The mean free path is obscure in such systems. The effect of boundaries is of much more importance in a granular system than in an elastic one. The asymmetric local velocity distribution implies the local mean free paths of positive and negative are different. Our results support this original hypothesis.

5. Conclusion

In this study, we focus on the local free path of vibrated granular gases through event-driven molecular dynamic simulation. The results demonstrate the local free path of granular gases is very different from the classical prediction. The probability distribution of the free path does not follow an exponential distribution expected by the classical elastic kinetic theory. Instead, anisotropy of the free path is found where the non-vibrating direction component of the probability of free path lengths is still exponential, while the vibrating direction component has a high tail. The probability distribution of angle between the relative velocity and the unit vector directed two particle centers disagrees with the distribution of two random vectors. Using the two-peak velocity distribution, we provide an expression of the free path based on the kinetic theory, which shows the local free path is related not only to the number density, but also to the granular temperature. The two-peak model results agree well with simulation, demonstrating the effect of non-equilibrium distribution. Future work will be directed to the experimental measurement of the free path and the mechanism underlying the two-peak distribution.

References

[1] Campbell C S 1990 *Ann. Rev. Fluid Mech.* **22** 57
[2] Goldhirsch I 2003 *Ann. Rev. Fluid Mech.* **35** 267
[3] Nichol K, Daniels K E 2012 *Phys. Rev. Lett.* **108** 018001
[4] Wang W and Chen Y P 2015 *Advances in Chemical Engineering*, Chapter Four, *Mesoscale Modeling: Beyond Local Equilibrium Assumption for Multiphase Flow* (Academic Press) pp. 193–277
[5] Puglisi A, Loreto V, Marconi U M B, Petri A and Vulpiani A 1998 *Phys. Rev. Lett.* **81** 3848
[6] Losert W, Cooper D G W, Delour J, Kudrolli A and Gollub J P 1999 *Chaos* **9** 682
[7] Olafsen J S and Urbach J S 1999 *Phys. Rev. E* **60** R2468
[8] Brey J J, Ruiz-Montero M J and Moreno F 2000 *Phys. Rev. E* **62** 5339
[9] Herbst O, Muller P, Otto M and Zippelius A 2004 *Phys. Rev. E* **70** 051313
[10] Chen Y P, Evesque P and Hou M Y 2014 *Engineering Computations* **32** 1066
[11] Chen Y P, Evesque P and Hou M Y 2012 *Chin. Phys. Lett.* **29** 074501
[12] Chen Y P, Hou M Y, Jiang Y M and Liu M 2014 *Phys. Rev. E* **88** 052204
[13] Brilliantov N V and Pöschel T 2004 *Kinetic Theory of Granular Gases* (New York: Oxford University Press) pp. 12–15
[14] Vincenti W G and Kruger C H 1956 *Introduction to Physical Gas Dynamics* (New York: John Wiley and Sons) pp. 12–15
[15] Kadanoff L P 1999 *Rev. Mod. Phys.* **71** 435
[16] Grossman E L, Zhou Tong and Ben-Naim E 1991 *Phys. Rev. E* **55** 4200
[17] Blair D L and Kudrolli A 2003 *Phys. Rev. E* **67** 041301
[18] Visco P, van Wijland F and Trizac E 2008 *Phys. Rev. E* **77** 041117
[19] Coppex F, Droz M and Trizac E 2004 *Phys. Rev. E* **69** 011303
[20] Tan M L and Goldhirsch I 1998 *Phys. Rev. Lett.* **81** 3022
[21] Dufty J W and Brey J J 1999 *Phys. Rev. Lett.* **82** 4566
[22] Tan M L and Goldhirsch I 1999 *Phys. Rev. Lett.* **82** 4567
[23] Glasser B J and Goldhirsch I 2001 *Phys. Fluids* **13** 407
[24] Cai T, Fan J and Jiang T 2013 *The Journal of Machine Learning Research* **14** 1837
[25] Mei Y, Chen Y and Wang W 2015 "Kinetic theory of binary particles with unequal mean velocities and non-equipartition energies" (arXiv:1508.02871)
[26] Chapman S and Cowling T G 1970 *The Mathematical Theory of Non-uniform Gases* (Cambridge: Cambridge University Press) pp. 89–99